Gear shifting based on MIMO model predictive control for convenient adjustment of shifting performance

Jinrak Park, and Seibum Choi, *Member, IEEE,*

***Abstract*—When shifting gears, it is necessary to properly adjust the gear shift time and the Maximum Variation of Output shaft Torque (MVOT) which are related to gear shift performance. At this time, the gear shift time and MVOT are related to the clutch slip speed and the output shaft torque, which can be controlled by the engine torque and clutch torque. Therefore, in order to adjust the gear shift performance, it is necessary to perform Multi-Input-Multi-Output (MIMO) control. In MIMO control, the system output is the clutch slip speed and output shaft torque, and the system input is the engine torque and clutch torque. In the past, several trajectories of the engine torque and clutch torque have been generated heuristically to adjust the gear shift performance. Therefore, a MIMO control method that is capable of adjusting the gear shift performance conveniently with a few tuning parameters during gear shifting is needed. In this study, a gear shift controller for generating target driveline torque (engine and clutch torque) based on MIMO model predictive control that can adjust the gear shift performance with only one tuning parameter is proposed. The gear shift controller proposed in this study is verified experimentally on a test bench equipped with a production dual-clutch transmission.**

***Index Terms*—Gear shift control, Clutch control, Transmission control, Model predictive control, Dual clutch transmission**

I. Introduction

WHEN shifting gears, the gear shift time and the Maximum Variation of the Output shaft Torque(MVOT) should be properly adjusted. At this time, the gear shift time is related to the clutch friction energy loss and vehicle drivability. Generally, the longer the gear shift time , the greater the frictional energy loss ($\int_0^{t_f} T_c\omega_{slip}dt$). And, since the output shaft torque is controlled by the vehicle Electronic Control Unit (ECU) during gear shifting and the driver cannot directly control the output shaft torque, the driver can feel uncomfortable if the gear shift time is long. In addition, the larger MVOT ($\dot{T}_o$), the greater the maximum vehicle jerk ($\dot{a}_x$) [1], [2]. Here, T_c, ω_{slip}, t_f, T_o, and a_x are the clutch torque, clutch slip speed, gear shift time, output shaft torque, and vehicle acceleration. Hereinafter, the ratio between the gear shift time and MVOT is referred to as the gear shift performance.

Fig. 1 shows the driveline state information during gear shifting of a dual clutch transmission (DCT). Figs. 1(a), (b), and (c) show the driveline speed, driveline torque, and output shaft torque, respectively.

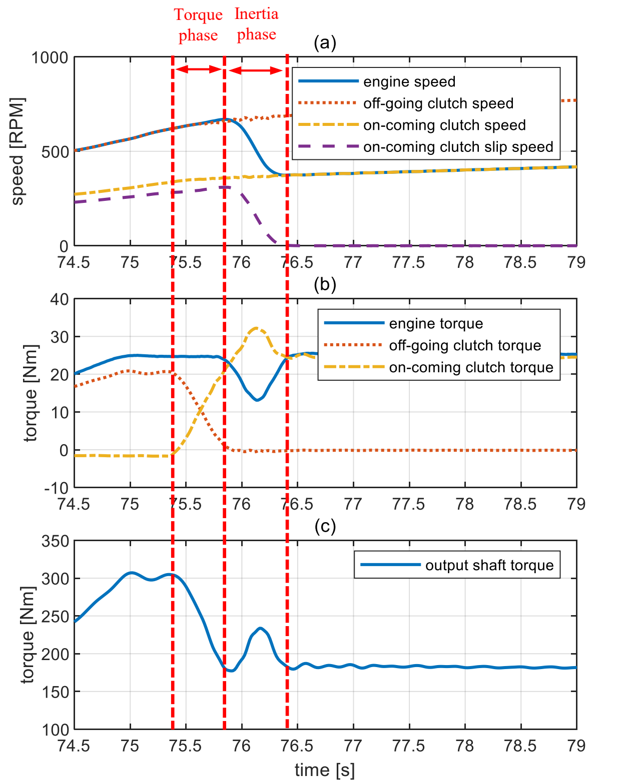

Fig. 1. Driveline state information during gear shifting of DCT: (a) driveline speed, (b) driveline torque, (c) output shaft torque.

Generally, in gear shifting of a DCT, the clutch that was engaged before gear shifting is called the off-going clutch, and the clutch that is engaged during gear shifting is called the on-coming clutch.

Referring to Fig. 1, the gear shift process of a DCT can be roughly divided into two phases [3]–[6].

The first phase is the torque phase in which the on-coming clutch brings the torque transmitted by the off-going clutch while the on-coming clutch is slip-engaged. Thus, in the torque phase, both the off-going clutch and on-coming clutch transmit torque, the off-going clutch torque decreases, and the on-coming clutch torque increases.

The second phase is the inertia phase in which the engine speed decreases and the on-coming clutch speed increases,

Jinrak Park and Seibum Choi are with KAIST, Daejeon 34141, South Korea (e-mail: pjr1413@kaist.ac.kr; sbchoi@kaist.ac.kr).

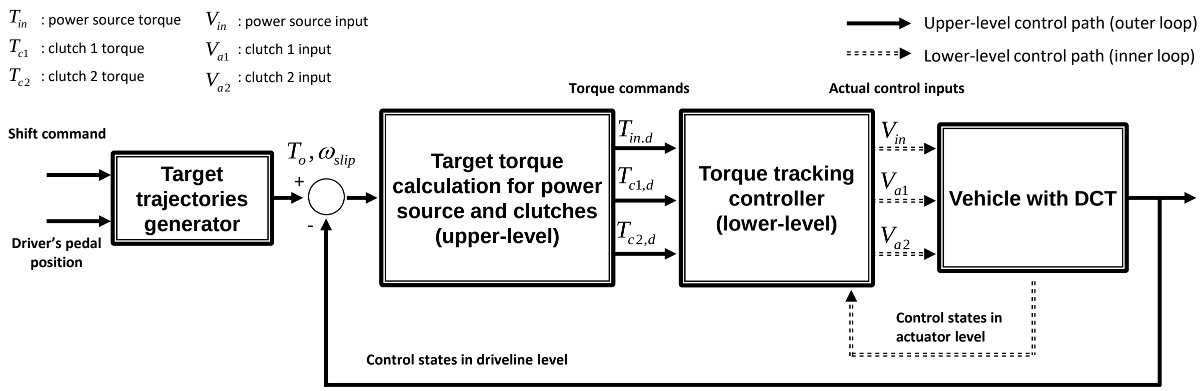

Fig. 2. Structure of gear shift control of DCT.

resulting in speed synchronization between the engine and the on-coming clutch.

After the on-coming clutch is fully engaged after gear shifting, the variation of the on-coming clutch slip speed is zero. So, in order for the gear shift inertia phase and the clutch-complete engagement phase to be continued smoothly, the variation of the on-coming clutch slip speed should be zero right before the clutch-complete engagement.

Referring to the slip speed dynamics equation of the on-coming clutch which will be mentioned in Section II, if the variation of the on-coming clutch slip speed is not close to zero right before the clutch-complete engagement, the clutch-complete engagement occurs in the condition that the difference between the engine torque and the on-coming clutch torque is large. At this time, since the on-coming clutch torque follows the engine torque due to the mechanical connection after the clutch-complete engagement, there is a large variation of the on-coming clutch torque after the clutch-complete engagement. In this process, the driveline torque vibration occurs, which can be directly felt by the driver. So, the control, to make the variation of the on-coming clutch slip speed to zero right before the clutch-complete engagement to reduce the driveline torque vibration after the clutch-complete engagement, is called smooth landing control of the slip speed.

The gear shifting covered in this study refers to the inertia phase in the gear shifting phase of a DCT. Hereinafter, unless otherwise specified, the clutch slip speed and clutch torque of the on-coming clutch are referred to as just the clutch slip speed and clutch torque, respectively.

On the other hand, referring again to the driveline dynamics equations which will be mentioned in Section II, the gear shift time and MVOT during gear shifting can be adjusted by controlling the clutch slip speed and output shaft torque. And, the slip speed is again controlled by the engine torque and clutch torque, and the output shaft torque is controlled by the clutch torque [7]–[15].

Therefore, in order to adjust the gear shift performance, it is necessary to perform Multi-Input-Multi-Output (MIMO) control. In the MIMO control, the system output is the clutch slip speed and output shaft torque, and the system input is the engine torque and clutch torque.

On the other hand, during gear shifting, the gear shift time and MVOT are in a trade-off relationship. This is because, in order to reduce the slip speed to zero quickly, the clutch torque should be increased, resulting in increased output shaft torque and MVOT [16], [17].

In the past, several trajectories of the engine torque and clutch torque have been generated heuristically to adjust the gear shift performance during gear shifting [18]–[21]. However, the tuning load to generate the trajectories of the engine torque and clutch torque for gear shifting in all situations is very large. Therefore, a MIMO control method that is capable of adjusting the gear shift performance conveniently with a few tuning parameters during gear shifting is needed.

Fig. 2 shows the general structure of gear shift control of a DCT. Referring to Fig. 2, the structure of the gear shift control can be largely divided into three parts generally.

The first part is the tracking control part of the engine torque and clutch torque when the target engine torque and clutch torque are given. Hereinafter, the first part of the gear shift control is referred to as the lower-level controller of gear shifting.

The second part is the control part that generates the target engine torque and clutch torque when the target clutch slip speed and output shaft torque are given. Hereinafter, the second part of the gear shift control is referred to as the upper-level controller of gear shifting.

Finally, the third part is the control part that generates the target clutch slip speed and output shaft torque that satisfies specific gear shift performance according to purposes of gear shifting. Hereinafter, the third part of the gear shift control is referred to as the target trajectory generator of gear shifting.

Regarding the research on the lower-level controller, a number of studies have been conducted on engine torque tracking control [22]–[25] and clutch torque tracking control [26]–[32].

Regarding the research of the upper-level controller, a number of studies have been conducted on the tracking control of the clutch slip speed [33]–[35], and few studies have been conducted on the multivariable tracking control [1], [2] of the clutch slip speed and output shaft torque.

Regarding the research of the target trajectory generator, a study has been conducted on the target trajectory generator of the clutch slip speed [17]. On the other hand, few studies have been conducted on the target trajectory generator of the clutch slip speed and output shaft torque during gear shifting.

Regarding the research that combines the upper-level controller and the target trajectory generator, in the study [16], a method of generating the target engine torque and clutch torque during gear shifting was proposed using the virtual input consisting of the current slip speed and the ideal output shaft torque. Hereinafter, the control part that combines the upper-level controller and the target trajectory generator is referred to as the integrated upper-level controller.

In the study [16], the gear shift performance could be adjusted with one tuning parameter. However, it was not clear what the virtual input meant, because the desired virtual input was calculated differently from the original definition. Therefore, it was not clear what the control targets were when generating the target engine torque and clutch torque.

In this study, an integrated upper-level controller of gear shifting is proposed based on MIMO Model Predictive Control (MPC) that can adjust the gear shift performance with only one tuning parameter. Also, this controller can implement the smooth landing control of the clutch slip speed by considering the constraint of the future slip speed. By performing the smooth landing control, it is possible to fully engage the clutch without large driveline torque vibration after the clutch-complete engagement even in fast gear shifting.

The integrated upper-level controller proposed in this study was verified by applying it to the first to second gear shift situation on a test bench equipped with a driving motor and a DCT of production parallel hybrid vehicles.

The main features of the integrated upper-level controller proposed in this study are as follows.

1. The control targets are clear.

2. The gear shift performance can be adjusted using one tuning parameter.

3. It is possible to generate a target trajectory of the engine torque and clutch torque considering the constraint of the system input and output.

4. It can implement the smooth landing control of the clutch slip speed.

5. There is no need to estimate the road load torque in detail when shifting gears.

This paper is organized as follows. Section 2 describes the driveline model of the test bench used in this study. Section 3 introduces the integrated upper-level controller based on MIMO MPC proposed in this study. Section 4 deals with the experimental results of the integrated upper-level controller on the test bench. Section 5 concludes this paper.

II. Driveline model

As mentioned in the introduction section, in order to properly adjust the gear shift performance, it is necessary to control the slip speed and output shaft torque. In this section, the driveline model of the test bench for the slip speed and output shaft torque is addressed.

Fig. 3 shows the structure of the test bench used in this study. The test bench was built such that the driveline of the test bench was as similar as possible to that of production vehicles. A driving motor and a DCT of production parallel hybrid vehicles were used on the test bench, and the motor was used to replace the engine of production vehicles. Hereinafter, the motor for driving the test bench is referred to as an engine.

Fig. 4 shows the schematic diagram of the lumped inertia driveline model of the test bench.

In this study, the driveline of the test bench is modeled using lumped inertias, and this driveline model can be used as a driveline model for production vehicles [7]–[15].

In the driveline of production vehicles, only the engine speed, odd gear clutch speed, even gear clutch speed, and wheel speed are generally measured, and only the speeds mentioned were also measured in the test bench.

Hereinafter, the odd gear clutch is referred to as clutch1, and the even gear clutch is referred to as clutch2 or just clutch.

This study focuses on the inertia phase in the first to second gear shifting process. In this case, the clutch1 is completely disengaged, and torque is not transmitted from the clutch1. And, the clutch2 is slip-engaged.

Referring to Fig. 4, the following equations can be obtained by establishing the torque balance equation at the measurement positions of the engine speed, clutch2 speed, and wheel speed and deriving the dynamic equation of the rotational speed [7]–[15].

$$\dot{\omega}_e = -\frac{1}{J_e} d_e \omega_e + \frac{1}{J_e} T_e - \frac{1}{J_e} T_{c1} - \frac{1}{J_e} T_{c2} \tag{1}$$

$$\dot{\omega}_{c2} = -\frac{1}{J_{eq2}} d_{eq2} \omega_{c2} + \frac{1}{J_{eq2}} i_{c2} i_{f2} T_{c2} - \frac{1}{J_{eq2}} T_o \tag{2}$$

$$\dot{\omega}_w = -\frac{1}{J_v} d_w \omega_w + \frac{1}{J_v} T_o - \frac{1}{J_v} T_r \tag{3}$$

where ω, d, J, T, and i are the rotational speed, shaft damping coefficient, lumped rotational inertia, torque, and gear ratio, and the subscripts e, $c2$, $f2$, o, and r denote the engine, even gear clutch, final gear connected to the even gear clutch, output shaft, and road load, and J_{eq2}, and d_{eq2} are the equivalent inertia at the clutch2 position including the inertias between the clutch2 and output shaft, and the equivalent damping coefficient at the clutch2 position including the damping effect between the clutch2 and output shaft, respectively.

In this study, the method of calculating the equivalent inertia and equivalent damping coefficient is not covered in detail for the sake of brevity. That method was covered in the studies [7]–[15].

In addition, by combining equations (2) and (3), the following equation can be derived.

$$\begin{aligned} \dot{\omega}_{c2} &= -\frac{[d_{eq2} + \frac{1}{i_{c2} i_{f2}} d_w]}{[J_{eq2} + \frac{1}{i_{c2} i_{f2}} J_v]} \omega_{c2} \\ &+ \frac{1}{[J_{eq2} + \frac{1}{i_{c2} i_{f2}} J_v]} i_{c2} i_{f2} T_{c2} - \frac{1}{[J_{eq2} + \frac{1}{i_{c2} i_{f2}} J_v]} T_r \end{aligned} \tag{4}$$

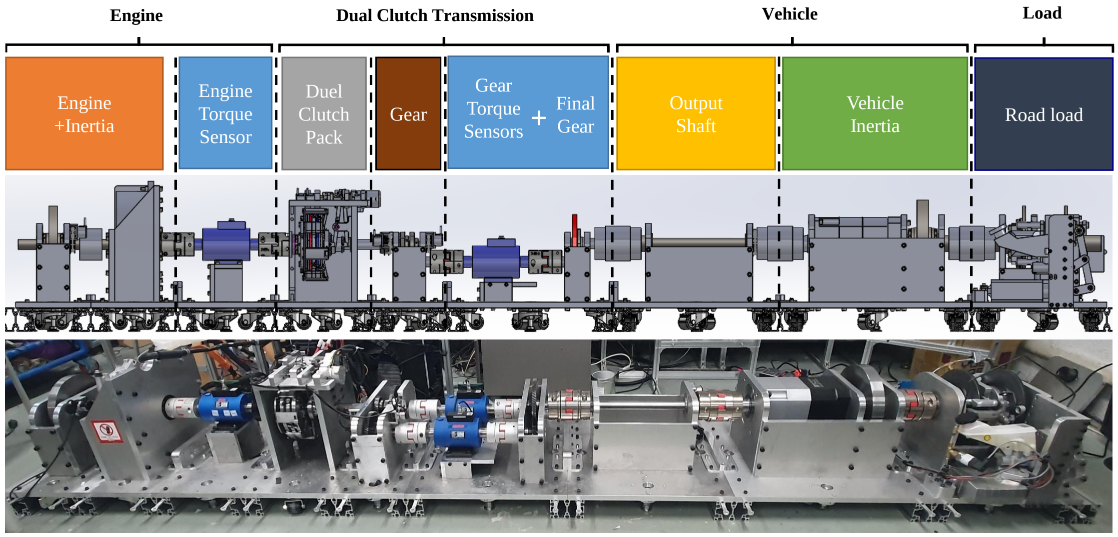

Fig. 3. Structure of the test bench.

Here, by combining equations (1) and (4), the slip speed dynamics equation of the clutch can be derived.

$$\begin{aligned}&\dot{\omega}_{slip2} = \dot{\omega}_e - \dot{\omega}_{c2}\\ &= [-\frac{d_e}{J_e} + \frac{[d_{eq2}+\frac{1}{i_{c2}i_{f2}}d_w]}{[J_{eq2}+\frac{1}{i_{c2}i_{f2}}J_v]}]\omega_e - \frac{[d_{eq2}+\frac{1}{i_{c2}i_{f2}}d_w]}{[J_{eq2}+\frac{1}{i_{c2}i_{f2}}J_v]}(\omega_e - \omega_{c2})\\ &+\frac{1}{J_e}T_e - [\frac{1}{J_e} + \frac{1}{[J_{eq2}+\frac{1}{i_{c2}i_{f2}}J_v]}i_{c2}i_{f2}]T_{c2}\\ &+\frac{1}{[J_{eq2}+\frac{1}{i_{c2}i_{f2}}J_v]}T_r\end{aligned} \tag{5}$$

where the subscript $slip2$ means the clutch2 slip speed.

In addition, referring to equation (2), assuming that the influence of the inertia torque is small in the relationship between the clutch torque and output shaft torque, the following equation can be obtained.

$$T_o = -d_{eq2}\omega_e + d_{eq2}(\omega_e - \omega_{c2}) + i_{c2}i_{f2}T_{c2} \tag{6}$$

Here, referring to equations (1), (5), and (6), a governing equation of a control system in the form of the state space can be derived as follows. Also, the system input is the engine torque and clutch torque and the system output is the clutch slip speed and the output shaft torque.

$$\begin{aligned}&\dot{\mathbf{x}}' = \mathbf{A}_c\mathbf{x}' + \mathbf{B}_c\mathbf{u} + \mathbf{E}_c\\ &\mathbf{y}' = \mathbf{C}_c\mathbf{x}' + \mathbf{D}_c\mathbf{u}\\ &\mathbf{u} = \begin{bmatrix} T_e \\ T_{c2}\end{bmatrix}, \mathbf{x} = \begin{bmatrix} \omega_e \\ \omega_{slip2}\end{bmatrix}, \mathbf{y}' = \begin{bmatrix} \omega_{slip2} \\ T_o\end{bmatrix}\\ &\mathbf{A_c} = \begin{bmatrix} -\frac{d_e}{J_e} & 0 \\ -\frac{d_e}{J_e} + \frac{[d_{eq2}+\frac{1}{i_{c2}i_{f2}}d_w]}{[J_{eq2}+\frac{1}{i_{c2}i_{f2}}J_v]} & -\frac{[d_{eq2}+\frac{1}{i_{c2}i_{f2}}d_w]}{[J_{eq2}+\frac{1}{i_{c2}i_{f2}}J_v]}\end{bmatrix},\\ &\mathbf{B_c} = \begin{bmatrix} \frac{1}{J_e} & -\frac{1}{J_e} \\ \frac{1}{J_e} & -[\frac{1}{J_e} + \frac{1}{[J_{eq2}+\frac{1}{i_{c2}i_{f2}}J_v]}i_{c2}i_{f2}]\end{bmatrix}\\ &\mathbf{C_c} = \begin{bmatrix} 0 & 1 \\ -d_{eq2} & d_{eq2}\end{bmatrix}, \mathbf{D_c} = \begin{bmatrix} 0 & 0 \\ 0 & i_{c2}i_{f2}\end{bmatrix},\\ &\mathbf{E_c} = \begin{bmatrix} 0 \\ [J_{eq2} + \frac{1}{i_{c2}i_{f2}}J_v]T_r\end{bmatrix}\end{aligned} \tag{7}$$

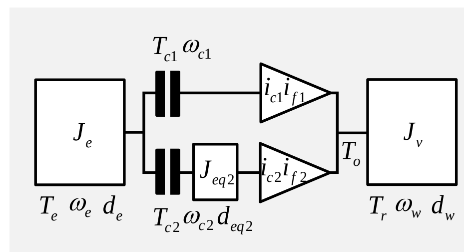

Fig. 4. Schematic diagram of a lumped inertia driveline model of an DCT vehicle.

TABLE I
PARAMETERS OF THE DRIVELINE MODEL

Parameter	Value	Parameter	Value
$J_e,\ kg \cdot m^2$	0.135	$d_e,\ kg \cdot m^2/s$	0.02
$J_{eq2},\ kg \cdot m^2$	0.2524	$d_{eq2},\ kg \cdot m^2/s$	0.4074
$J_v,\ kg \cdot m^2$	142.4289	$d_w,\ kg \cdot m^2/s$	0.001
$i_{c1}, -$	100/26	$i_{f1}, -$	100/25
$i_{c2}, -$	80/40	$i_{f2}, -$	100/24
$m_v,\ kg$	1583	$r_w,\ m$	0.3

Converting equation (7) to a digital system, the following equation can be derived.

$$\begin{aligned}&\mathbf{x}'(k+1) = \mathbf{A_d}\mathbf{x}'(k) + \mathbf{B_d}\mathbf{u}(k) + \mathbf{E_d}\\ &\mathbf{y}'(k) = \mathbf{C_d}\mathbf{x}'(k) + \mathbf{D_d}\mathbf{u}(k)\\ &\mathbf{A_d} = e^{\mathbf{A_c}T_s},\ \mathbf{B_d} = \int_0^{T_s} e^{\mathbf{A_c}\tau}ds \cdot \mathbf{B}_c,\\ &\mathbf{E}_d = \int_0^{T_s} e^{\mathbf{A_c}\tau}ds \cdot \mathbf{E_c}\\ &\mathbf{C_d} = \mathbf{C_c},\ \mathbf{D_d} = \mathbf{D_d}\end{aligned} \tag{8}$$

Table I shows the parameters of the driveline model used in this study.

III. GEAR SHIFT CONTROL USING MODEL PREDICTIVE CONTROL

In this section, the integrated upper-level controller based on MIMO MPC proposed is described. In this study, the MPC

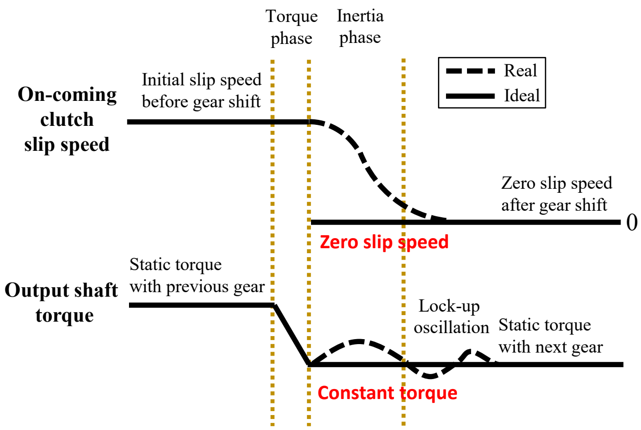

Fig. 5. Real and ideal trajectories of the clutch slip speed and output shaft torque during gear shifting.

method based on the Laguerre functions was used to reduce the computational load of MPC, and the literature [36] was referred for the MPC method. In the MPC method based on the Laguerre functions, the optimal input is expressed as a weighted sum of the Laguerre functions, and the computational load can be reduced by reducing the number of the optimization variables from the number of the future prediction step to the number of Laguerre functions. On the other hand, if an ECU can cover the computational load, the MPC method using Laguerre functions may not necessarily be used for the gear shift control, but a general MPC method can be used. The method mentioned below can be applied to a general MPC method through slight modifications.

A. Control target

Fig. 5 shows the real and ideal trajectories of the clutch slip speed and output shaft torque during gear shifting.

Referring to Fig. 5, in order to reduce the gear shift time during gear shifting which is related to the clutch friction energy loss and vehicle drivability, it is desirable to reduce the slip speed to zero as quickly as possible.

In addition, when gear shifting starts, using the initial value of the engine torque, and the gear ratio information of shafts connected to the on-coming clutch, the output shaft torque can be predicted after gear shifting [1], [2]. Furthermore, in order to reduce MVOT during gear shifting which is related to the vehicle jerk, it is desirable to keep the output shaft torque constant as the predicted output shaft torque.

Therefore, it can be seen that the ideal value of the slip speed and output shaft torque is known when gear shifting starts. Hereinafter, the ideal value of the slip speed and output shaft torque during gear shifting is referred to as the ideal slip speed and output shaft torque. And, This ideal slip speed and output shaft torque are utilized as the control target in the later section.

B. Augmented predictive model

When predicting the future system output in a MPC method, a governing equation can be used as it is, but the variation of the governing equation can also be used.

When predicting the future system output, the variation of the governing equation can be used to reduce the output error caused by the disturbance of the system.

The road load torque varies greatly depending on vehicle air resistance, rolling resistance, and gradient resistance, but does not change within a short time.

In general, it can be assumed that the road load torque does not change during the gear shift time because the gear shift time is quite short, within a few seconds.

Therefore, the E_d term related to the road load torque in the system governing equation of equation (8) can be regarded as the disturbance of the system.

In this study, a method that predicts the clutch slip speed and output shaft torque in the future using the variation of the governing equation is utilized. At this time, when predicting the clutch slip speed and output shaft torque in the future, if the governing equation is used as it is without using the variation of the governing equation, an additional estimator to estimate the road load torque is required.

Referring to equation (8), by establishing a future prediction model using the variation of the governing equation, it can be derived as follows.

$$\begin{aligned}
&\mathbf{x}(k+1) = \mathbf{A}\mathbf{x}(k) + \mathbf{B}_1\Delta\mathbf{u}(k) + \mathbf{B}_2\Delta\mathbf{u}(k+1) \\
&\mathbf{y_e}(k) = \mathbf{C}\mathbf{x}(k) \\
&\Delta\mathbf{u} = \begin{bmatrix} \Delta T_e \\ \Delta T_{c2} \end{bmatrix}, \mathbf{x} = \begin{bmatrix} \Delta\mathbf{x}' \\ \mathbf{y}' - \mathbf{y}'_{\mathbf{target}} \end{bmatrix} \\
&\mathbf{y_e} = \mathbf{y}' - \mathbf{y}'_{\mathbf{target}} \\
&\mathbf{y}'_{\mathbf{target}} = \begin{bmatrix} \omega_{slip.target} \\ T_{o.target} \end{bmatrix} \\
&\mathbf{A} = \begin{bmatrix} \mathbf{A_d} & \mathbf{0} \\ \mathbf{C_d A_d} & \mathbf{I} \end{bmatrix}, \mathbf{B_1} = \begin{bmatrix} \mathbf{B_d} \\ \mathbf{C_d B_d} \end{bmatrix}, \mathbf{B_2} = \begin{bmatrix} \mathbf{0} \\ \mathbf{D_d} \end{bmatrix} \\
&\mathbf{C} = \begin{bmatrix} \mathbf{0} & \mathbf{I} \end{bmatrix}
\end{aligned} \tag{9}$$

where $\mathbf{y}'_{\mathbf{target}}$, $\omega_{slip2.target}$, and $T_{o.target}$ is the system control target, target clutch slip speed, and target output shaft torque.

On the other hand, in a general MPC method, if there is a system input term in the output formula, as shown in equation (8), the future output cannot be predicted and the controller cannot be designed. This is because the future input is needed to predict the future output.

So, in this study, we propose to use the following assumption related to the system input.

$$\Delta\mathbf{u}(k-1) \approx \Delta\mathbf{u}(k) \tag{10}$$

In this case, equation (9) is modified as follows.

$$\begin{aligned}
&\mathbf{x}(k+1) = \mathbf{A}\mathbf{x}(k) + \mathbf{B}\Delta\mathbf{u}(k) \\
&\mathbf{y_e}(k) = \mathbf{C}\mathbf{x}(k) \\
&\Delta\mathbf{u} = \begin{bmatrix} \Delta T_e \\ \Delta T_{c2} \end{bmatrix}, \mathbf{x} = \begin{bmatrix} \Delta\mathbf{x}' \\ \mathbf{y}' - \mathbf{y}'_{\mathbf{target}} \end{bmatrix} \\
&\mathbf{y_e} = \mathbf{y}' - \mathbf{y}'_{\mathbf{target}} \\
&\mathbf{A} = \begin{bmatrix} \mathbf{A_d} & \mathbf{0} \\ \mathbf{C_d A_d} & \mathbf{I} \end{bmatrix}, \mathbf{B} = \begin{bmatrix} \mathbf{B_d} \\ \mathbf{C_d B_d} + \mathbf{D_d} \end{bmatrix} \\
&\mathbf{C} = \begin{bmatrix} \mathbf{0} & \mathbf{I} \end{bmatrix}
\end{aligned} \tag{11}$$

If the assumption of equation (10) is used, there is an effect that the clutch torque is calculated one step in advance when

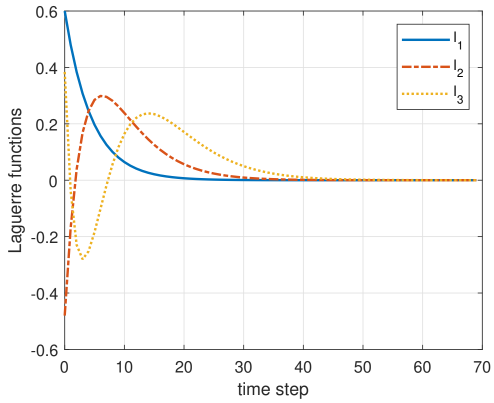

Fig. 6. Example shape of the Laguerre functions in the time domain when N=3 and α=0.8.

calculating the clutch torque for producing specific output shaft torque.

However, as mentioned in the introduction section, the goal of the integrated upper-level controller based on MIMO MPC covered in this study is not to improve the absolute tracking performance of the clutch slip speed and output shaft torque for the ideal clutch slip speed and output shaft torque during gear shifting. Rather, the goal is to make the tracking performance relatively different according to some tuning parameters.

Therefore, calculating the clutch torque one step ahead does not significantly affect the relative tracking performance according to the tuning parameters.

C. System input expression using Laguerre functions

In the MPC method based on the Laguerre functions, the system input is expressed as a weighted sum of the Laguerre functions that satisfy orthonormality in the time domain as follows.

$$\begin{aligned}
&\Delta u_i(k+m) = \mathbf{L}_i(m)^T \eta_i \\
&\mathbf{L}_i(k)^T = \left[\begin{array}{cccc} l_1^i(k) & l_2^i(k) & \cdots & l_N^i(k) \end{array}\right] \\
&\eta_i = \left[\begin{array}{cccc} c_1^i & c_1^i & \cdots & c_N^i \end{array}\right]^T \\
&\Delta u_1 = \Delta T_e,\, \Delta u_2 = \Delta T_{c2}
\end{aligned} \tag{12}$$

where l, η, and N means the Laguerre function, Laguerre coefficient, and the number of the Laguerre functions, and the subscript i is a symbol that identifies each input.

Laguerre functions in the time domain are expressed as follows.

$$\begin{aligned}
&\mathbf{L}_i(0)^T \\
&= \sqrt{\beta_i}\left[\begin{array}{cccccc} 1 & -\alpha_i & \alpha_i^2 & -\alpha_i^3 & \cdots & (-1)^{N-1}\alpha_i^{N-1} \end{array}\right] \\
&\beta = (1-\alpha_i^2),\, (0<\alpha_i<1) \\
&\mathbf{L}_i(k+1) = \mathbf{A}_l^i \mathbf{L}_i(k) \\
&\mathbf{A}_l^i = \left[\begin{array}{ccccc} \alpha_i & 0 & 0 & 0 & \cdots \\ \beta_i & \alpha_i & 0 & 0 & \cdots \\ -a_i\beta_i & \beta_i & \alpha_i & 0 & \cdots \\ \alpha_i^2\beta_i & -\alpha_i\beta_i & \beta_i & \alpha_i & \cdots \\ \vdots & \vdots & \vdots & \vdots & \ddots \end{array}\right]
\end{aligned} \tag{13}$$

where α is a tuning parameter. α is the pole of the discrete-time Laguerre network, and the value is between 0 and 1. And, this parameter is related to the shape of the Laguerre functions in the time domain.

If the tuning parameter N is large, the Laguerre functions can catch the trajectory of the system input in detail. But, N has a great influence on the computational load of MPC since N is related to the number of optimization variables. So, it should be appropriately selected according to the ECU performance. Also, α should be chosen to achieve appropriate control performance for a given N. Details related to the tuning of N and α are covered in more detail in the result section.

Fig. 6 shows an example shape of the Laguerre functions in the time domain when N=3 and α=0.8.

Finally, the system input consisting of the engine torque and clutch torque is expressed as follows using the Laguerre functions.

$$\begin{aligned}
&\Delta \mathbf{u}(k+m) = \mathbf{L}(m)^T \eta \\
&\mathbf{L}(m)^T = \left[\begin{array}{cc} \mathbf{L_1}(m)^T & 0 \\ 0 & \mathbf{L_2}(m)^T \end{array}\right] \\
&\eta^T = \left[\begin{array}{cc} \eta_1^T & \eta_2^T \end{array}\right]
\end{aligned} \tag{14}$$

D. Prediction of the system state and output

Using equations (11), and (14), the future system state and output can be predicted using the following equations.

$$\begin{aligned}
&\mathbf{x}(k+m|k) = \mathbf{A}^m \mathbf{x}(k) + \sum_{j=0}^{m-1} \mathbf{A}^{m-j-1}\mathbf{B}\mathbf{L}(j)^T \eta \\
&= \mathbf{A}^m \mathbf{x}(k) + \varphi(m)^T \eta \\
&\varphi(m)^T = \sum_{j=0}^{m-1} \mathbf{A}^{m-j-1}\mathbf{B}\mathbf{L}(j)^T \\
&\mathbf{y}_e(k+m|k) = \mathbf{C}\mathbf{x}(k+m|k)
\end{aligned} \tag{15}$$

E. Optimization problem

In this study, the cost function in the MPC method consists of the control error(system output) of the clutch slip speed and output shaft torque, and the variation of the system input as follows.

$$\begin{aligned}
J &= \sum_{m=1}^{N_p} \left[\begin{array}{c} \mathbf{y}_e(k+m|k)^T \bar{\mathbf{Q}} \mathbf{y}_e(k+m|k) \\ +\Delta\mathbf{u}(k+m-1)^{\mathbf{T}} \mathbf{R} \Delta\mathbf{u}(k+m-1) \end{array}\right] \\
&= \sum_{m=1}^{N_p} \left[\begin{array}{c} \mathbf{x}(k+m|k)^T \mathbf{Q} \mathbf{x}(k+m|k) \\ +\Delta\mathbf{u}(k+m-1)^{\mathbf{T}} \mathbf{R} \Delta\mathbf{u}(k+m-1) \end{array}\right] \\
\bar{\mathbf{Q}} &= \left[\begin{array}{cc} q_1 & 0 \\ 0 & q_2 \end{array}\right],\, \mathbf{Q} = \mathbf{C}^T \bar{\mathbf{Q}} \mathbf{C},\, \mathbf{R} = \left[\begin{array}{cc} r_1 & 0 \\ 0 & r_2 \end{array}\right]
\end{aligned} \tag{16}$$

where N_p is the length of the prediction horizon, and $\bar{\mathbf{Q}}$, and $\mathbf{R}$ are tuning parameters.

This study aims at the smooth landing control of the slip speed as well as the adjustment of the gear shift performance during gear shifting. Therefore, the length of the predicted horizon N_p should be selected as a time sufficient to implement the smooth landing control in the operating range of the slip speed according to the constraint of the system input. The method to calculate suitable N_p is covered in the later section.

In the tuning parameter $\bar{\mathbf{Q}}$, q_1 and q_2 are the parameters to adjust the ratio of the control error of the clutch slip speed and output shaft torque in the cost function. And, in the tuning parameter $\mathbf{R}$, r_1 and r_2 are the parameters to adjust the ratio of the variation of each system input in the cost function. In this study, we propose a method to adjust the gear shift performance by fixing $\mathbf{R}$ as a unitary matrix and adjusting $\bar{\mathbf{Q}}$ appropriately.

Details related to the tuning of N_p, and $\bar{\mathbf{Q}}$ are covered in more detail in the result section.

Here, using the orthnormality characteristics of the Laguerre functions, and (14), the above equations can summarized as follows.

$$J = \sum_{m=1}^{N_p} [\mathbf{x}(k+m|k)^T \mathbf{Q}\mathbf{x}(k+m|k)] + \eta^T \mathbf{R}\eta \tag{17}$$

Substituting the equation (15) to the above equation and arranging it, the following equation can be obtained.

$$\begin{aligned} & J = \eta^T \mathbf{\Omega}\eta + 2\eta^T \mathbf{\Psi}\mathbf{x}(k) \\ & + \sum_{m=1}^{N_p} \mathbf{x}(k)^T (\mathbf{A}^T)^m \mathbf{Q}\mathbf{A}^m \mathbf{x}(k) \\ & \mathbf{\Omega} = \left(\sum_{m=1}^{N_p} \varphi(m)\mathbf{Q}\varphi(m)^T + \mathbf{R} \right) \\ & \mathbf{\Psi} = \left(\sum_{m=1}^{N_p} \varphi(m)\mathbf{Q}\mathbf{A}^m \right) \end{aligned} \tag{18}$$

For a unconstrained problem, the optimal solution η to minimize the equation (18) can be summarized as follows after differentiating the equation (18) for η.

$$\eta = -\mathbf{\Omega}^{-1}\mathbf{\Psi}\mathbf{x}(k) \tag{19}$$

Here, for a unconstrained problem, the optimal feedback control gain is summarized as follows using equations (14) and (19).

$$\begin{aligned} & \Delta\mathbf{u}(k) = -\mathbf{K_{mpc}}\mathbf{x}(\mathbf{k}) \\ & \mathbf{K_{mpc}} = \mathbf{L}(0)\mathbf{\Omega}^{-1}\mathbf{\Psi} \end{aligned} \tag{20}$$

Substituting the equation (19) to the equation (18), the optimal cost can be summarized as follows.

$$\begin{aligned} & J_{\min} = \mathbf{x}^T(k) P_{mpc} \mathbf{x}(k) \\ & P_{mpc} = \left(\sum_{m=1}^{N_p} (\mathbf{A}^T)^m \mathbf{Q}\mathbf{A}^m - \mathbf{\Psi}^T \mathbf{\Omega}^{-1}\mathbf{\Psi} \right) \end{aligned} \tag{21}$$

the equations (20), and (21) are utilized to tune the tuning parameter N, α, and $\bar{\mathbf{Q}}$ in the later result section.

On the other hand, for a constrained problem, since the last term in the equation (18) is not related to the future information of the system, the cost function to be finally minimized is defined as follows.

$$\begin{aligned} & J = \eta^T \mathbf{H}\eta + 2\eta^T \mathbf{f} \\ & \mathbf{H} = \mathbf{\Omega} \\ & \mathbf{f} = \mathbf{\Psi}\mathbf{x}(k) \end{aligned} \tag{22}$$

In this study, the following values are used as the target clutch slip speed and output shaft torque. These values are the ideal target value of the clutch slip speed and output shaft torque mentioned in the introduction section.

$$\begin{aligned} & \omega_{slip2.target} = 0 \\ & T_{o.target} = i_{c2} i_{f2} T_{e.init} \end{aligned} \tag{23}$$

where $T_{e.init}$ is the initial engine torque at the beginning of the gear shift inertia phase.

In equation (22), the output shaft torque included in state $\mathbf{x}$ in the f term corresponding to measurement feedback is not measured. Therefore, in this study, the output shaft torque was calculated as follows by using the model equation of equation (6).

$$T_o(k) = -d_{eq2}\omega_e + d_{eq2}(\omega_e - \omega_{c2}) + i_{c2} i_{f2} T_{c2}(k-1) \tag{24}$$

In this way, when the output shaft torque is calculated using the model equation, some control error corresponding to the model error may occur when controlling the output shaft torque.

F. Constraint of the system input and output

In this study, the following constraint on the system input and output are considered.

$$\begin{aligned} & \Delta\mathbf{u}^{\min} \leq \Delta\mathbf{u}(k) \leq \Delta\mathbf{u}^{\max} \\ & \mathbf{u}^{\min} \leq \mathbf{u}(k) \leq \mathbf{u}^{\max} \\ & \mathbf{y}^{\min} \leq \mathbf{y}(k) \leq \mathbf{y}^{\max} \end{aligned} \tag{25}$$

Constraint for the future system input and output can be expressed as follows.

$$\begin{aligned} & \Delta\mathbf{U}^{\min} \leq \Delta\mathbf{U}(k) \leq \Delta\mathbf{U}^{\max} \\ & \mathbf{U}^{\min} \leq \mathbf{U}(k) \leq \mathbf{U}^{\max} \\ & \mathbf{Y}^{\min} \leq \mathbf{Y}(k) \leq \mathbf{Y}^{\max} \\ & \Delta\mathbf{U}^{\min} = \left[\begin{array}{ccc} \Delta\mathbf{u}^{\min} & \cdots & \Delta\mathbf{u}^{\min}(N_c-1) \end{array} \right]^T \\ & \Delta\mathbf{U}^{\max} = \left[\begin{array}{ccc} \Delta\mathbf{u}^{\max} & \cdots & \Delta\mathbf{u}^{\max}(N_c-1) \end{array} \right]^T \\ & \mathbf{U}^{\min} = \left[\begin{array}{ccc} \mathbf{u}^{\min} & \cdots & \mathbf{u}^{\min}(N_c-1) \end{array} \right]^T \\ & \mathbf{U}^{\max} = \left[\begin{array}{ccc} \mathbf{u}^{\max} & \cdots & \mathbf{u}^{\max}(N_c-1) \end{array} \right]^T \\ & \mathbf{Y}_e^{\min} = \left[\begin{array}{ccc} \mathbf{y}_e^{\min} & \cdots & \mathbf{y}_e^{\min}(N_p-1) \end{array} \right]^T \\ & \mathbf{Y}_e^{\max} = \left[\begin{array}{ccc} \mathbf{y}_e^{\max} & \cdots & \mathbf{y}_e^{\max}(N_p-1) \end{array} \right]^T \end{aligned} \tag{26}$$

where N_c is the length of the control horizon.

The length of the control horizon N_c corresponds to the length of the future system input to which the constraint is to be applied, and it is set to be less than the length of the prediction horizon. On the other hand, if the length of the control horizon is short, the system output is predicted without taking into account the constraint of the future system input. Therefore, the future prediction may not be effective, and the system control performance may decrease since it is difficult to respond in advance if pre-reaction is required to achieve control objectives. Whereas, if the length of the control horizon is long, the system control performance may improve, but the computational load increases. In this study, the same length of the prediction horizon and control horizon is used to ensure maximum system control performance.

Referring to the equation (14), the variation of the system input can be expressed as follows.

$$\begin{aligned} & \Delta\mathbf{U}(k) = \mathbf{M}_1\eta(k) \\ & \mathbf{M}_1 = \left[\begin{array}{cccc} \mathbf{L}(0)^T & \mathbf{L}(1)^T & 0 & \mathbf{L}(N_p-1)^T \end{array} \right]^T \end{aligned} \tag{27}$$

Also, the future system input can be expressed as follows.

$$\begin{aligned}&\mathbf{U}(k)=\mathbf{M}_2\eta(k)+\mathbf{M}_3\mathbf{u}(k-1)\\&\mathbf{M}_2=\\&\left[\begin{array}{cccc}\mathbf{L}(0)^T & \mathbf{L}(0)^T+\mathbf{L}(1)^T & \cdots & \sum_{m=1}^{N_c}\mathbf{L}(m-1)^T\end{array}\right]^T\\&\mathbf{M}_3=\left[\begin{array}{ccc}\mathbf{I} & \cdots & \mathbf{I}\end{array}\right]^T\end{aligned} \tag{28}$$

Furthermore, referring to the equations (15), and (26), the future system output can be expressed as follows.

$$\begin{aligned}&\mathbf{Y}_e=\mathbf{M}_4\eta(k)+\mathbf{M}_5\mathbf{x}(k)\\&\mathbf{M}_4\\&=\left[\begin{array}{cccc}\left(\mathbf{C}\phi(1)^T\right)^T & \left(\mathbf{C}\phi(2)^T\right)^T & \cdots & \left(\mathbf{C}\phi(N_p)^T\right)^T\end{array}\right]^T\\&\mathbf{M}_5=\left[\begin{array}{cccc}(\mathbf{CA})^T & \left(\mathbf{CA}^2\right)^T & \cdots & \left(\mathbf{CA}^m\right)^T\end{array}\right]^T\end{aligned} \tag{29}$$

Finally, referring to the equations (26), (27), (28), and (29), the constraint matrix can be summarized as follows.

$$\begin{aligned}&\mathbf{M}\eta\leq\gamma\\&\mathbf{M}=\begin{bmatrix}\mathbf{M}_1\\-\mathbf{M}_1\\\mathbf{M}_2\\-\mathbf{M}_2\\\mathbf{M}_4\\-\mathbf{M}_4\end{bmatrix},\ \gamma=\begin{bmatrix}\Delta\mathbf{U}^{\max}\\-\Delta\mathbf{U}^{\min}\\\mathbf{U}^{\max}+\mathbf{M}_3\mathbf{u}(k-1)\\-\mathbf{U}^{\min}-\mathbf{M}_3\mathbf{u}(k-1)\\\mathbf{Y}^{\max}+\mathbf{M}_5\mathbf{x}(k)\\-\mathbf{Y}^{\min}-\mathbf{M}_5\mathbf{x}(k)\end{bmatrix}\end{aligned} \tag{30}$$

G. Linear quadratic problem

Finally, to calculate the MPC control input, a Linear Quadratic (LQ) Program using equations (22) and (30) should be solved. In this study, the quadprog tool provided in MATLAB was used to solve the LQ problem. In this paper, the method of solving the LQ problem is not covered in detail.

IV. Experimental results

The main objectives of the integrated upper-level controller were to properly adjust the gear shift performance according to the tuning parameter $\bar{\mathbf{Q}}$, and to implement the smooth landing of the slip speed. In this section, the integrated upper-level controller based on MIMO MPC proposed in this study is verified through the experiments of the first to second gear shifting. Also, it is verified whether two main objectives are properly achieved.

A. Experimental environment

As mentioned in Section II, a test bench was used to verify the integrated upper-level controller. Fig. 3 shows the structure of the test bench used in this study.

The test bench was built so that the driveline of the test bench was as similar as possible to that of production vehicles. A driving motor and a DCT of production parallel hybrid vehicles were used on the test bench, and the motor was used to replace of an engine of production vehicles.

In addition, the first gear was connected to the clutch1, and the second gear was connected to the clutch2.

Furthermore, MicroAutobox2 from the dSpace company was used as a ECU. The control loop time(sampling time) was set to 15 milliseconds in consideration of the computational load of MPC, and the MPC operated smoothly in the control loop.

Referring to Fig. 3, regarding the measurement on the test bench, the engine speed, clutch1 speed, clutch2 speed, and wheel speed were measured, and the DCT input shaft torque, first gear final shaft torque, and second gear final shaft torque were measured. In the figures below, the measured engine torque, clutch1 torque, clutch2 torque, output shaft torque, and road load torque were calculated using the mentioned measured torque and taking into account shaft inertias. The method of calculating the measured torque is omitted for the sake of brevity.

B. Parameter selection

In this study, the control loop time was basically 15 milliseconds in consideration of the computational load of MPC.

And, the following constraint of the variation of the system input were used. The unit of the variation of the system input is Nm/s.

$$\Delta\mathbf{u}_{\min}=\left[\begin{array}{cc}-1 & -1\end{array}\right]^T,\ \Delta\mathbf{u}_{\max}=\left[\begin{array}{cc}1 & 1\end{array}\right]^T \tag{31}$$

In addition, regarding to the constraint of the system input, only the minimum constraint was applied to the engine torque and clutch torque to reduce the computational load of MPC as follows. the following equations can be derived by appropriately modifying the equations (26), and (30). The unit of the system input is Nm.

$$T_{c2.min}=(T_{c2.init}-2),\ T_{e.min}=0 \tag{32}$$

where $T_{c2.init}$ is the initial clutch torque at the beginning of the gear shift inertia phase.

Furthermore, regarding to the constraint of the system output, the minimum constraint was applied to only the clutch slip speed for the smooth landing control of the slip speed as follows. This constraint makes the variation of the slip speed to zero when the slip speed reaches zero. The unit of the slip speed is RPM/s.

$$\omega_{slip2.e}^{\min}=0 \tag{33}$$

where $\omega_{slip2.e}$ is the control error of the clutch slip speed.

And, there were several tuning parameters mentioned before. It was the length of the prediction horizon N_p, the number of the Laguerre functions N, the shape parameter of the Laguerre functions α, and the penalty factor of the control error $\bar{\mathbf{Q}}$.

Fig. 7 shows the variation of the ideal engine torque and clutch torque from the initial torque, and the variation of the slip speed from the initial speed accordingly when the gear shift inertia phase starts with the initial variation of the slip speed of 0, and the future prediction is possible for 0.3 seconds.

In the figure, 0 represents the initial torque and speed, and the initial torque and speed are different for each gear shifting situation. In addition, each value represents the variation from the initial value. Here, the equation (5) was utilized to calculate

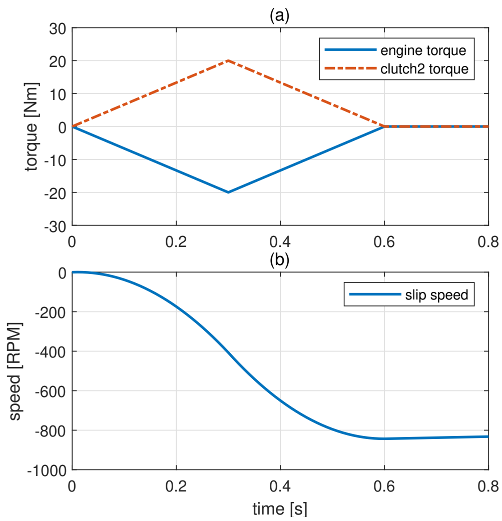

Fig. 7. Variation of the ideal engine torque and clutch torque from the initial torque and the variation of the slip speed from the initial speed accordingly.

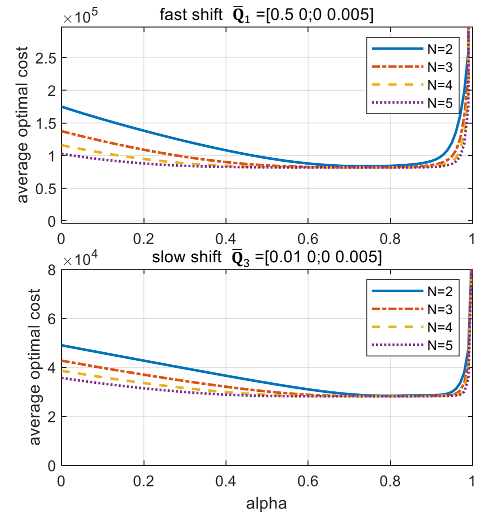

Fig. 8. Average optimal cost according to several different initial system state when $\bar{\mathbf{Q}}$, N, and α are different.

the variation of the slip speed, and the road load torque T_r was assumed to be 100Nm.

Referring to Fig. 7, if the future prediction is possible up to for 0.3 seconds in the conditions that T_r is 100Nm and the constraint of the engine torque and clutch torque is considered as equations (31) and (32), it can be seen that the smooth landing control is possible up to the initial slip speed is about 800 RPM. This slip speed roughly corresponds to the slip speed when the engine speed is about 1500RPM and the first to second gear shifting occurs.

For example, for a given system input constraint and maximum value of T_r, the slip speed trajectory can be drawn using the slip speed dynamics equation depending on several candidates of the length of the future prediction horizon. Then, if the absolute value of the minimum slip speed is greater than the desired maximum initial slip speed, it means that the smooth landing control is possible under the relevant condition. Using this analysis method, the minimum length of the future prediction horizon can be calculated.

In this study, the proposed integrated upper-level controller is verified in the first to second gear shifting under the conditions of the initial slip speed of approximately 400RPM and T_r of approximately 100Nm.

Referring to Fig. 7, considering the performance of the ECU used in this study, it was determined that 0.3 seconds of the future prediction was sufficient for the mentioned experimental conditions. So, considering that the control loop time was 15 milliseconds, N_p was chosen as 20 steps. The length of the control horizon N_c was chosen the same as N_p in this study. In a real application, N_p may be longer.

Fig. 8 shows the average optimal cost according to several different initial system state when $\bar{\mathbf{Q}}$, N, and α are different. In this study, the same N was used for all system input for convenience. And, the values between $\bar{\mathbf{Q}}_\mathbf{1}$ =[0.5, 0;0, 0.005] and $\bar{\mathbf{Q}}_\mathbf{3}$ =[0.01, 0;0, 0.005] were used as $\bar{\mathbf{Q}}$, and the optimal cost was calculated using the boundary values of $\bar{\mathbf{Q}}$. The initial system state was set by dividing each state 5 intervals in the range of -1000< $\dot{\omega}_e$ <0RPM/s, -1000< $\dot{\omega}_{slip2}$ <0RPM/s, 0< ω_{slip2} <3000RPM/s, and 0< T_o <500Nm. And, the optimal cost was calculated using the equation (21).

At this time, the system input, generated as a result of optimization, converges to a specific input trajectory if the input is expressed in detail according to N and α. Then, the optimal cost does not decrease further according to N and α but converges to a specific value. At this time, if the optimal cost for a specific N and α is not significantly different from the convergent optimal cost, it means that the Laguerre functions of the specific N and α are sufficient to express the system input. Here, since N has a great influence on the computational load of MPC, a small N can be selected so that the difference between the optimal cost and the convergent optimal cost is not large. Similarly, for α, a value between 0 and 1 is selected so that the difference between the optimal cost and the convergent optimal cost is not large.

Referring to Fig. 8, it can be seen that the difference is not large between the optimal cost when N is 3 and α is 0.8, and the convergent optimal cost when the N is larger. Thus, in this study, 3, and 0.8 were used as N, and α, respectively, and the shape of the Laguerre functions are shown in Fig. 6.

Fig. 9 shows the closed loop bode plot of the control error of the slip speed and output shaft torque depending on the different tuning parameter $\bar{\mathbf{Q}}$. In the figure, the x-axis means the input frequency of the target control error, and the y-axis means the ratio between the target control error and the actual control error.

The following equations were derived using the equations (11) and (20), and it was used to represent the closed loop bode plot.

$$\begin{aligned}
&\Delta\mathbf{u}(k) = \mathbf{K_{mpc}}[\mathbf{x}_{target}(k) - \mathbf{x}(k)] \\
&\mathbf{x}(k+1) = (\mathbf{A} - \mathbf{BK_{mpc}})\mathbf{x}(k) + \mathbf{BK_{mpc}}\mathbf{x}_{target}(k) \\
&\mathbf{y_e}(k) = \mathbf{Cx}(k)
\end{aligned} \tag{34}$$

In the above equations, $\mathbf{x}_{target}$ means the control target of the system state, and the control target of the system output

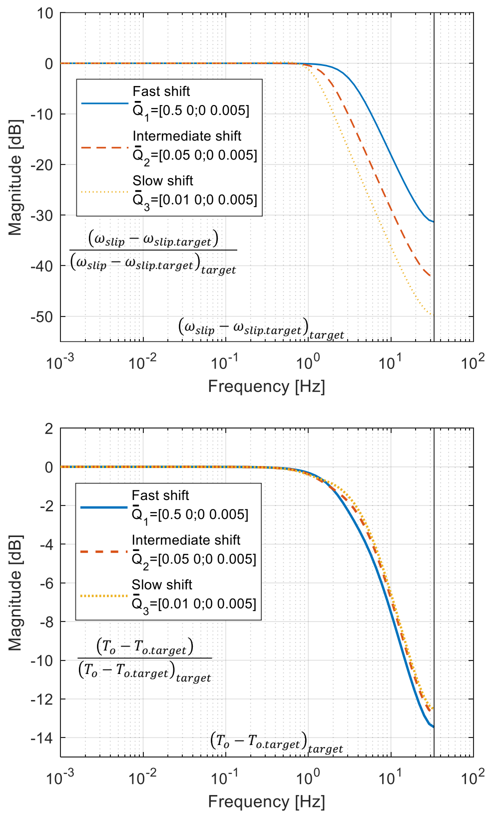

Fig. 9. Closed loop bode plot of the control error of the slip speed and output shaft torque depending on the different tuning parameter $\bar{\mathbf{Q}}$.

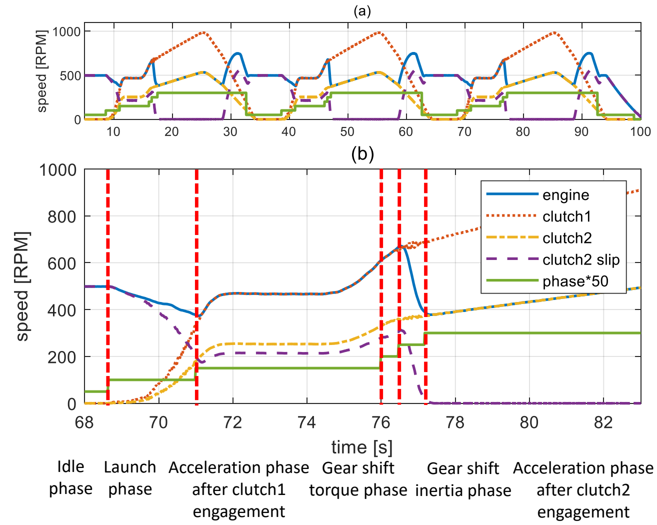

Fig. 10. Example of the driveline speed in the verification experiment of the integrated upper-level controller: (a) driveline speed for the entire experiment period, (b) driveline speed for the third launching and gear shifting.

was included in the system state. Here, the control target of the actual system state is all zero.

Referring to Fig. 9, the closed loop bandwidth of the control error of the slip speed and the output shaft torque was approximately [3.07Hz; 3.58Hz], [1.66Hz; 4.67Hz], and [1.22Hz; 4.86Hz], respectively when $\bar{\mathbf{Q}}$ was set to $\bar{\mathbf{Q}}_\mathbf{1}$ =[0.5, 0;0, 0.005, $\bar{\mathbf{Q}}_\mathbf{2}$ =[0.05, 0;0, 0.005], and $\bar{\mathbf{Q}}_\mathbf{3}$ =[0.01, 0;0, 0.005], respectively. At this time, the penalty factor of the variation of the system input $\mathbf{R}$ was fixed as a unitary matrix. For the mentioned $\bar{\mathbf{Q}}$, the closed loop poles of the control error were located inside the unit circle.

The actuator bandwidth of the engine torque and clutch torque of the test bench used in this study was approximately 5Hz, and in consideration of this, $\bar{\mathbf{Q}}$ was set such that the closed loop bandwidth of the control error was less than 5Hz.

Looking at the principle of the integrated upper-level controller proposed in this study with reference to equation (34), if the closed loop bandwidth of the control error of the output shaft torque is relatively larger than the closed loop bandwidth of the control error of the slip speed, the control error of the output shaft torque is converged to zero relatively earlier than the control error of the slip speed, resulting in the smaller MVOT.

Conversely, if the closed loop bandwidth of the control error of the slip speed is relatively larger than the closed loop bandwidth of the control error of the output shaft torque, the control error of the slip speed is converged to zero relatively earlier than the control error of the output shaft torque, resulting in the smaller gear shift time.

C. Experimental scenario

Fig. 10 shows an example of the driveline speed in the verification experiment of the integrated upper-level controller. Figs. 10(a), and (b) show the driveline speed for the entire experiment period and the driveline speed for the third launching and gear shifting, respectively.

In order to avoid duplication of information in the figure, the wheel speed is not shown, and the wheel speed can be calculated as the product of the clutch2 speed and the gear ratio($i_{c2}i_{f2}$).

Referring to Fig.10, vehicle launching and gear shifting were performed three times for each controller under different conditions, and the control results for the third gear shifting were compared with each other in the next subsections.

The phase value shown in the figures below is the value representing the detailed launch and gear shift phase, and phase values from 1 to 6 mean the idle phase, clutch1 slip engagement phase when the vehicle launches, vehicle acceleration and deceleration phase after clutch1 engagement, torque phase in gear shifting, inertia phase in gear shifting, and vehicle acceleration and deceleration phase after clutch2 engagement, respectively.

Fig. 11 shows an example of the target and measured driveline torque in the verification experiment of the integrated upper-level controller. Figs. 11(a), (b), (c), (d), (e), and (f) show the target and measured engine torque for the entire experiment period, the target and measured engine torque for the third launching and gear shifting, the target and measured clutch torque for the entire experiment period, the target and measured clutch torque for the third launching and gear shifting, the measured road load torque for the entire experiment period, and the measured road load torque for the third launching and gear shifting, respectively.

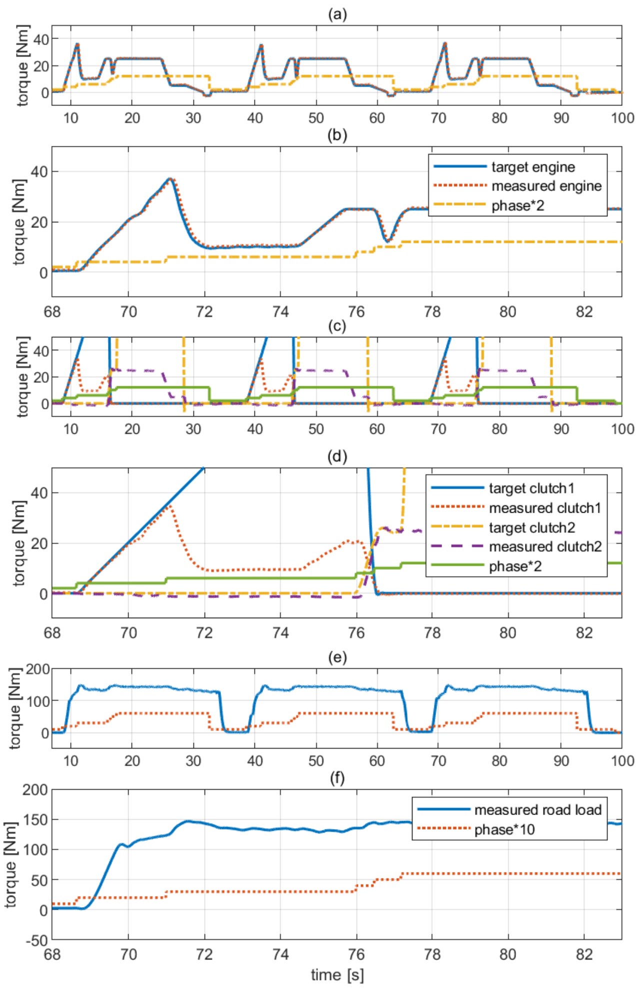

Fig. 11. Example of the target and measured driveline torque in the verification experiment of the integrated upper-level controller: (a) target and measured engine torque for the entire experiment period, (b) target and measured engine torque for the third launching and gear shifting, (c) target and measured clutch torque for the entire experiment period, (d) target and measured clutch torque for the third launching and gear shifting, (e) measured road load torque for the entire experiment period, (f) measured road load torque for the third launching and gear shifting.

In this study, the engine torque was feed-forward controlled using the relationship map between the driving motor current and engine torque, and the motor current was feedback-controlled using a current sensor.

In addition, the clutch torque was controlled in the adaptive feed-forward manner using the relationship map between the clutch actuator position and clutch torque [31], and the actuator position was feedback-controlled using a position sensor.

Since this study focuses on the integrated upper-level controller in gear shifting, the lower-level controller is not covered in detail. Meanwhile, depending on a system, before operating the integrated upper-level controller, the lower-level controller should be configured to operate properly.

Referring to Figs. 11(a), (b), (c), and (d), the engine torque and clutch torque were controlled to about 3Nm RMS error level that did not have a big problem to verify the integrated upper-level controller.

Referring to Figs. 11(e) and (f), the road load torque did not change significantly during gear shifting.

Furthermore, in this study, in the torque phase of gear shifting, the clutch1 torque increased linearly by the engine torque value at the beginning of the gear shifting, and the clutch2 torque decreased linearly according to the relationship of equation (1).

D. Landing control result of the clutch slip speed

Fig. 12 shows the driveline speed and target driveline torque before and after the landing control. Fig. 12(1st column), (2nd column), (1st row), and (2nd row) show the results before the landing control, the results after the landing control, the driveline speed, and the target driveline torque, respectively.

Fig. 13 shows the measured driveline torque, output shaft torque, and variation of the output shaft torque before and after the landing control. Fig. 13(1st column), (2nd column), (1st row), (2nd row), and (3rd row) shows the results before the landing control, the results after the landing control, the measured driveline torque, the target and measured output shaft torque, and the measured variation of the output shaft torque, respectively.

Hereinafter, for convenience, the landing control results before and after the slip speed constraint such as the equation (33) is considered in the equation (30) is referred to as the results before and after the landing control.

In this subsection, the experimental results before and after the landing control are comparatively analyzed for the same tuning parameter $\bar{\mathbf{Q}}$. In the next subsection, the experimental results of the gear shift control when the landing control is identically applied and only the tuning parameter $\bar{\mathbf{Q}}$ is different is analyzed.

The experimental scenario before and after the landing control was the same as previously mentioned. Also, the tuning parameter $\bar{\mathbf{Q}}$ was $\bar{\mathbf{Q}}_1$ and all the same parameters were used except that the slip speed constraint was considered in the experiments before and after the landing control.

When the clutch is fully engaged after gear shifting, the variation of the clutch slip speed is zero. Here, in order for the gear shift inertia phase and the complete clutch engagement phase to be continued smoothly, the variation of the slip speed should be zero at the end of the gear shift inertia phase.

As mentioned in the introduction section, referring to the equation (5), if the variation of the clutch slip speed is not close to zero right before the clutch-complete engagement, the clutch-complete engagement occurs in the condition that the difference between the engine torque and the clutch torque is large. At this time, since the clutch torque follows the engine torque due to the mechanical connection after the clutch-complete engagement, there is a large variation of the clutch torque after the clutch-complete engagement. In this process, the driveline torque vibration occurs, which can be directly felt by the driver.

Therefore, at the end of the gear shift inertia phase, the target engine torque and the clutch torque should become approximately the same in order to make the variation of the clutch slip speed to zero.

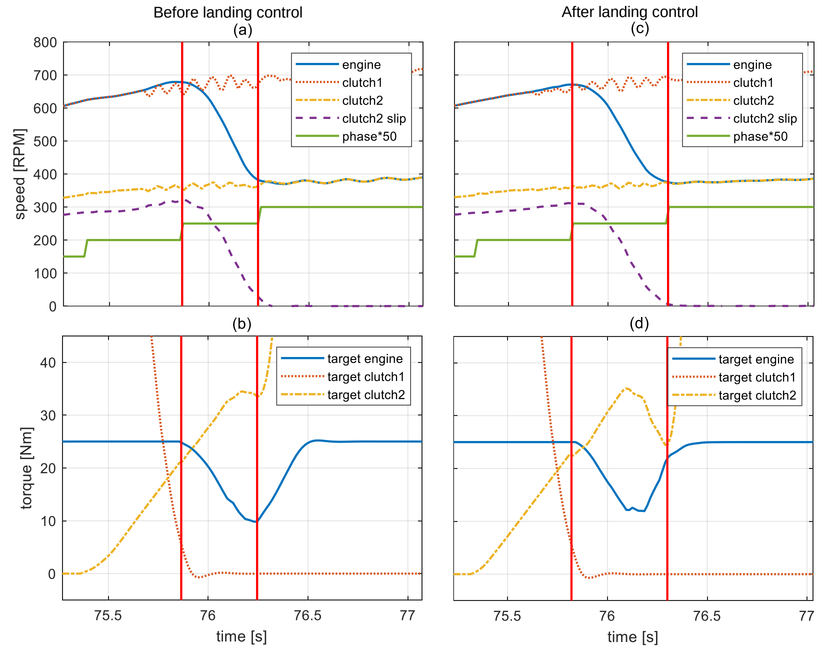

Fig. 12. Driveline speed and target driveline torque before and after the landing control: (1st column) results before the landing control, (2nd column) results after the landing control, (1st row) driveline speed, (2nd row) target driveline torque.

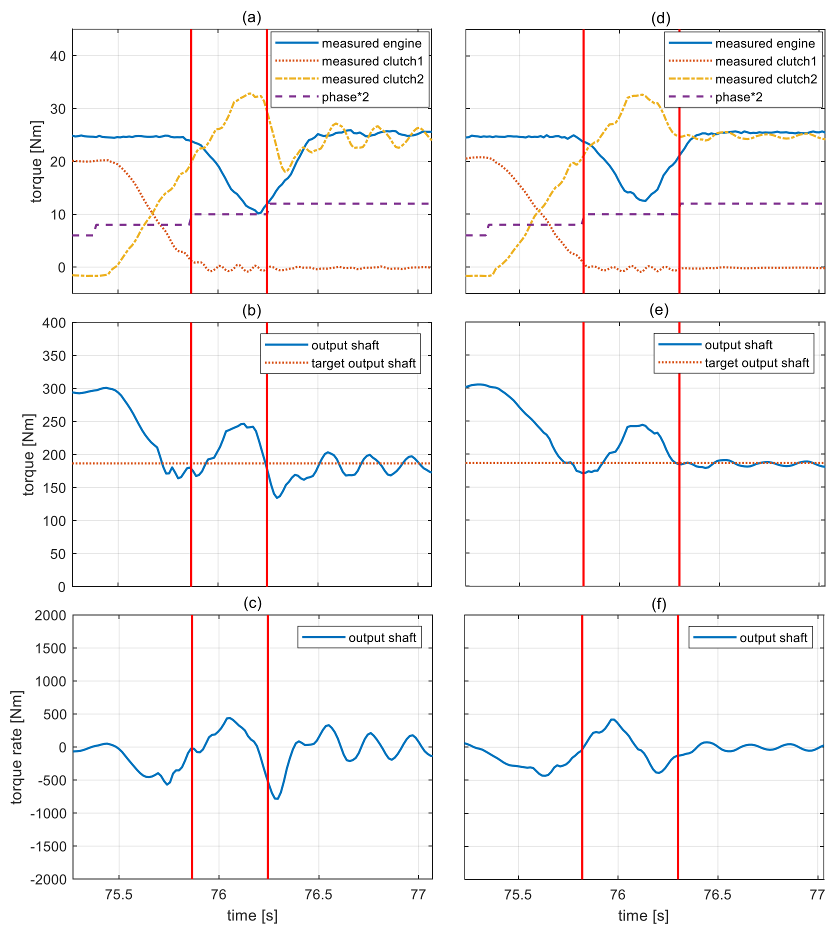

Fig. 13. Measured driveline torque, output shaft torque, and variation of the output shaft torque before and after the landing control: (1st column) results before the landing control, (2nd column) results after the landing control, (1st row) measured driveline torque, (2nd row) target and measured output shaft torque, (3rd row) measured variation of the output shaft torque.

TABLE II
GEAR SHIFT TIME, FRICTION ENERGY LOSS, MVOT, AND VEHICLE JERK BEFORE AND AFTER THE LANDING CONTROL

Landing control	Gear shift time(inertia phase) t_f [s]	Friction energy loss [J]	MVOT $\max\left\lvert\dot{T}_o\right\rvert$ $[Nm/s]$	Maximum vehicle jerk $\max\lvert\dot{a}_x\rvert$ $[m/s^2]$
Before	0.39	266.8	780.2	6.29
After	0.47	234.8	417.9	7.62

In this study, the slip speed constraint such as the equation (33) was considered in the equation (30) to make the variation of the clutch slip speed to zero at the end of the gear shift inertia phase.

Referring to Fig. 12(1st column), and Fig. 13(1st column), before the landing control, the clutch was fully engaged when the negative variation of the slip speed and the difference between the target engine torque and clutch torque were relatively large. As a result, the clutch torque and output shaft torque were dropped sharply after the complete clutch engagement and recovered. And, the negative variation of the output shaft torque was relatively large and the vibration of the clutch torque and output shaft torque was also relatively large after the clutch complete engagement.

On the other hand, before the landing control, the vibration after the clutch complete engagement is related to the closed loop bandwidth of the control error of the slip speed. Here, if the closed loop bandwidth is very small, the gear shift time may be increased but the engagement vibration after the complete engagement may be reduced. However, it is difficult to reduce the gear shift time and engagement vibration at the same time unless the landing control is performed.

On the other hand, since the MPC method can consider the hard constraint of the slip speed, it has the advantage that the landing control is possible which makes the variation of the slip speed to zero right before the clutch complete engagement even in fast gear shifting.

Referring to Fig. 12(2nd column), Fig. 13(2nd column), After the landing control, the clutch was fully engaged after the variation of the slip speed was reduced to close to zero, and when the difference between the target engine torque and clutch torque was relatively small. As a result, the clutch torque was smoothly landed to the engine torque after the complete engagement, so the variation of the output shaft torque was relatively small. Also, the output shaft torque was not dropped significantly compared to the target value and the vibration of the clutch torque and output shaft torque was relatively small after the complete engagement.

Table II shows the gear shift time, clutch friction energy loss, MVOT, and vehicle jerk before and after the landing control.

The clutch friction energy loss and vehicle jerk were calculated using the below equations.

$$\int_0^{t_f} T_{c2}\omega_{slip2}dt \tag{35}$$

$$m_v\dot{a}_x r_w = J_v\ddot{\omega}_w \tag{36}$$

where m_v, and r_w are the vehicle mass, and vehicle wheel radius. This parameters used were shown in Table I.

As mentioned in the introduction, this study mainly focuses on the inertia phase of the gear shifting, so the gear shift time in Table II and the next table means the duration of the inertia phase in the gear shifting.

Referring to Table II and Fig. 13(3rd column), it can be seen that when the landing control was performed, the gear shift time increased but MVOT decreased, relative to when the landing control was not performed. Also, the clutch friction energy loss increased but maximum vehicle jerk decreased.

Furthermore, it can be seen that the vibration of the engine torque, clutch torque, and output shaft torque was greatly reduced after the gear shifting was finished, and the variation of the output shaft torque was reduced as well.

E. Experimental results of the MPC control depending on the different tuning parameter $\bar{\mathbf{Q}}$

Fig. 14 shows the driveline speed and target driveline torque depending on the different tuning parameter $\bar{\mathbf{Q}}$. Fig. 10 (1st column), (2nd column), (3rd column), (1st row), and (2nd row) shows the results of the tuning parameter $\bar{\mathbf{Q}}_\mathbf{1}$, the results of the tuning parameter $\bar{\mathbf{Q}}_\mathbf{2}$, the results of the tuning parameter $\bar{\mathbf{Q}}_\mathbf{3}$, the driveline speed, and the target driveline torque, respectively.

Fig. 15 shows the measured driveline torque, output shaft torque, and variation of the output shaft torque depending on the different tuning parameter $\bar{\mathbf{Q}}$. Fig. 15(1st column), (2nd column), (3rd column), (1st row), (2nd row), and (3rd row) shows the results of the tuning parameter $\bar{\mathbf{Q}}_\mathbf{1}$, the results of the tuning parameter $\bar{\mathbf{Q}}_\mathbf{2}$, (3rd column) results of the tuning parameter $\bar{\mathbf{Q}}_\mathbf{3}$, the measured driveline torque, the target and measured output shaft torque, and the variation of the output shaft torque, respectively.

Fig. 14, and 15 show the results after considering the constraint of the slip speed like the equation (33) in the equation (30) for the smooth landing control of the slip speed, and these results show the difference depending on only the tuning parameter $\bar{\mathbf{Q}}$ without landing issue. And, the landing control results before and after considering the constraint of the slip speed in the condition of the same tuning parameter $\bar{\mathbf{Q}}$ were covered in the previous subsection.

Referring to Fig. 14(1st row), and Fig. 15(2nd row), it can be seen that the clutch slip speed and output shaft torque converged well to the ideal clutch slip speed and output shaft torque, which are the control targets of the integrated upper-level controller.

Also, referring to Fig. 14 and Fig. 15, it can be seen that, when $q_2 = 0.005$ of the tuning parameter $\bar{\mathbf{Q}}$, the smaller the q_1 value was, the longer the gear shift time was and the smaller MVOT was. In addition, the target engine torque and clutch torque were generated such that the gear shift time and MVOT were adjusted depending on the tuning parameter $\bar{\mathbf{Q}}$.

Table III shows the gear shift time, clutch friction energy loss, MVOT and vehicle jerk during gear shifting according to the different tuning parameter $\bar{\mathbf{Q}}$.

Referring to Table III, it can be seen that the gear shift time and MVOT were adjusted well depending on the tuning

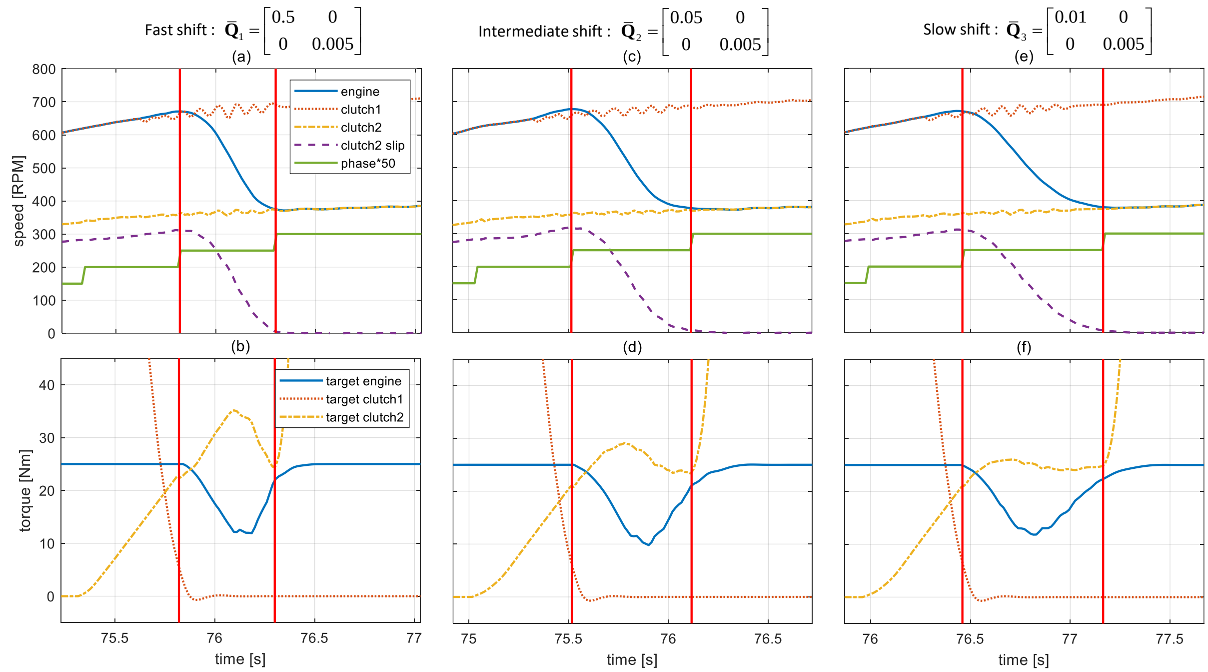

Fig. 14. Driveline speed and target driveline torque depending on the different tuning parameter $\bar{\mathbf{Q}}$: (1st column) the results of the tuning parameter $\bar{\mathbf{Q}}_1$, (2nd column) the results of the tuning parameter $\bar{\mathbf{Q}}_2$, (3 column) the results of the tuning parameter $\bar{\mathbf{Q}}_3$, (1st row) driveline speed, (2nd row) target driveline torque.

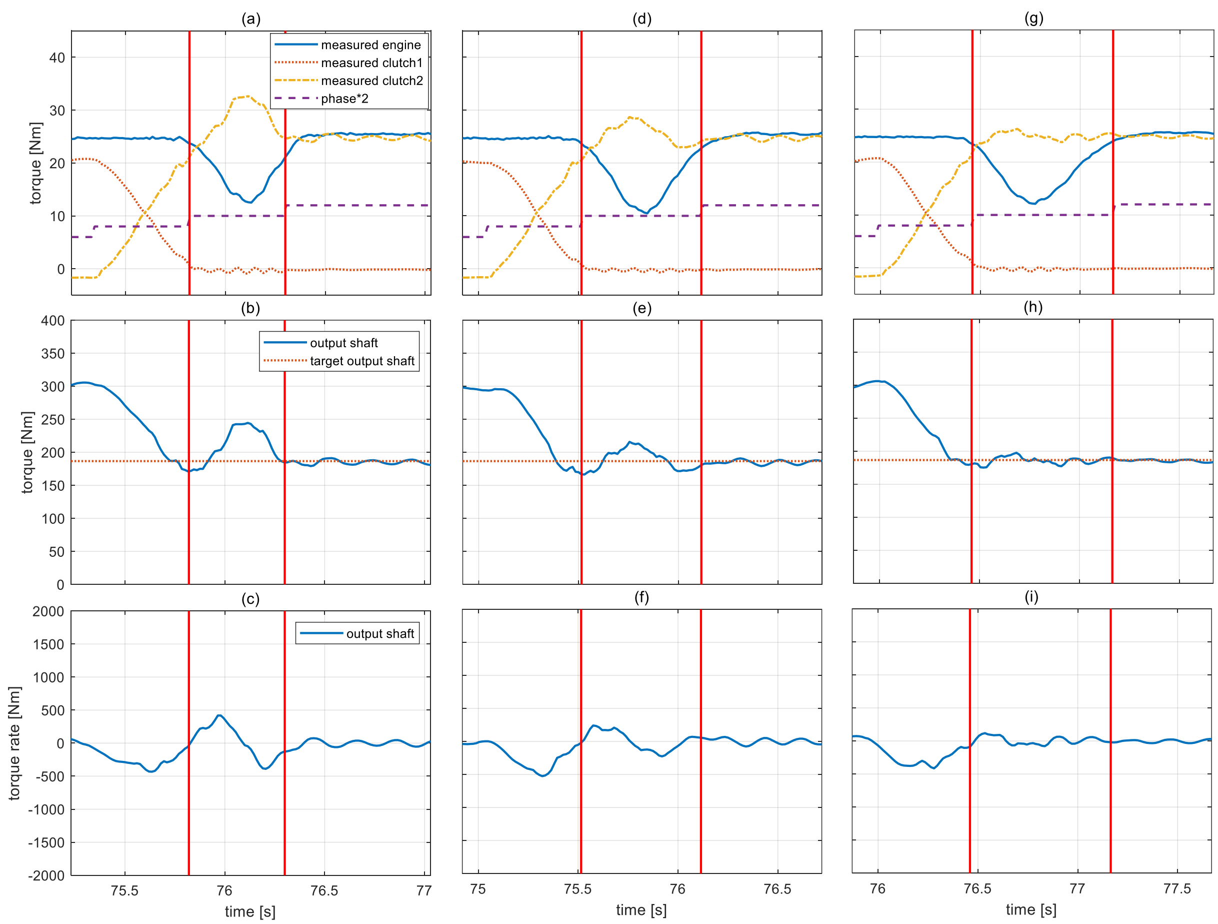

Fig. 15. Measured driveline torque, output shaft torque, and variation of the output shaft torque depending on the different tuning parameter $\bar{\mathbf{Q}}$: (1st column) results of the tuning parameter $\bar{\mathbf{Q}}_1$, (2nd column) results of the tuning parameter $\bar{\mathbf{Q}}_2$, (3rd column) results of the tuning parameter $\bar{\mathbf{Q}}_3$, (1st row) measured driveline torque, (2nd column) target and measured output shaft torque, (3rd row) the variation of the output shaft torque.

TABLE III
GEAR SHIFT TIME, FRICTION ENERGY LOSS, MVOT, AND VEHICLE JERK ACCORDING TO THE DIFFERENT TUNING PARAMETER $\bar{\mathbf{Q}}$

Tuning parameter $\bar{\mathbf{Q}}$	Gear shift time(inertia phase) t_f [s]	Friction energy loss [J]	MVOT $\max\left\|\dot{T}_o\right\|$ $[Nm/s]$	Maximum vehicle jerk $\max\left\|\dot{a}_x\right\|$ $[m/s^2]$
$\bar{\mathbf{Q}}_\mathbf{1}$	0.47	266.8	417.7	6.29
$\bar{\mathbf{Q}}_\mathbf{2}$	0.61	274.3	239.3	3.38
$\bar{\mathbf{Q}}_\mathbf{3}$	0.7	276.1	116.7	2.47

parameter $\bar{\mathbf{Q}}$, and thus the clutch friction energy loss and maximum vehicle jerk were also adjusted well.

Here, when q_2 is constant, what q_1 is small means that the error of the output shaft torque occupies a greater proportion in the cost function of equation (22) than the error of the clutch slip speed.

This also means that in the MIMO control, the target engine torque and clutch torque are generated such that the error of the output shaft torque can be reduced more rapidly than the error of the clutch slip speed.

Referring to equation (31), (32), and Fig. 14(2nd row), it can be seen that the target engine torque and clutch torque were generated appropriately by taking into account the constraint on the system input and the variation of the system input in the integrated upper-level controller.

In general, in order to reduce the gear shift time, it is necessary to reduce the engine torque as much as possible and increase the clutch torque as much as possible. On the other hand, the engine torque cannot be less than zero, and the variation of the engine torque is limited by the engine dynamics. In addition, since a large variation of the output shaft torque during gear shifting causes discomfort to the driver, the variation of the clutch torque during gear shifting is also limited.

In Fig. 14(b), it can be seen that the target engine torque and clutch torque were generated as close as possible to the constraint of the system input and the variation of the system input to reduce the gear shift time as much as possible.

On the other hand, it is desirable to shorten the gear shift time as much as possible after the ideal output shaft torque is achieved.

In Fig. 14(f), it can be seen that the target engine torque was appropriately reduced in order to reduce the gear shifting time as much as possible while the clutch torque corresponding to the ideal output shaft torque was kept constant.

In the results of this experiment, the clutch and wheel speeds did not change significantly since the road load torque was low and the vehicle inertia was large. However, if the clutch and wheel speeds change significantly, the slip speed will eventually converge to zero due to the convergence stability. However, some lagging of the convergence may occur depending on the constraint of the variation of the engine torque and clutch torque.

Furthermore, if needed, the target engine torque and clutch torque trajectories can also be adjusted by adjusting the constraint of the system input. In this study, the tuning parameters $\bar{\mathbf{Q}}$ and $\bar{\mathbf{R}}$ are determined by the closed loop bandwidth of the control target. However, the constraint of the system input can be determined by the actuator performance of the system input, but can be also freely modified according to the desired shape of the target system input.

In conclusion, in this study, the authors proposed an integrated upper-level controller based on MIMO MPC that can adjust the gear shift performance during gear shifting with only one tuning parameter, and it was experimentally verified. In addition, the problem that large driveline torque vibration occurred after the gear shifting was finished was solved by additionally performing the landing control.

V. CONCLUSION

In this study, an integrated upper-level controller of gear shifting based on MIMO MPC that can adjust the gear shift performance with only one tuning parameter. The major characteristics of the integrated upper-level controller proposed in this study was that the gear shift control was intuitive since the control variables were the clutch slip speed and output shaft torque which are directly related to the gear shift performance. Also, the target engine torque and the clutch torque trajectories could be generated in real time by considering the constraints of the control input and output variables. Especially, the smooth landing control was possible to reduce the vibration of the driveline torque after the clutch-complete engagement in consideration of the constraint that makes the variation of the slip speed to 0 right before the clutch-complete engagement. Furthermore, the road resistance torque was not used in the gear shift control by utilizing the variation of the governing equation. As a future work, a study to enhance the control robustness of the integrated upper-level controller will be conducted.

ACKNOWLEDGMENT

This research was partly supported by the National Research Foundation of Korea(NRF) grant funded by the Korea government(MSIP) (No. 2020R1A2B5B01001531), and the BK21+ program through the NRF funded by the Ministry of Education of Korea.

REFERENCES

[1] S. Kim and S. B. Choi, "Cooperative control of drive motor and clutch for gear shift of hybrid electric vehicles with dual-clutch transmission," *IEEE/ASME Transactions on Mechatronics*, 2020.

[2] G. Li and D. Görges, "Optimal control of the gear shifting process for shift smoothness in dual-clutch transmissions," *Mechanical Systems and Signal Processing*, vol. 103, pp. 23–38, 2018.

[3] Q. Gu and X.-s. Cheng, "Study on double-clutch transmission gear shift control based on optimal control theory," in *2011 IEEE 18th international conference on industrial engineering and engineering management*. IEEE, Conference Proceedings, pp. 629–634.

[4] J. Kim, K. Cho, and S. B. Choi, "Gear shift control of dual clutch transmissions with a torque rate limitation trajectory," in *Proceedings of the 2011 American Control Conference*. IEEE, Conference Proceedings, pp. 3338–3343.

[5] M. Kulkarni, T. Shim, and Y. Zhang, "Shift dynamics and control of dual-clutch transmissions," *Mechanism and Machine Theory*, vol. 42, no. 2, pp. 168–182, 2007.

[6] T. Minowa, H. Kimura, J. Ishii, S. Morinaga, T. Shiraishi, and N. Ozaki, "Smooth gear shift control system using estimated torque," *SAE transactions*, pp. 1427–1434, 1994.

[7] J. Kim, S. B. Choi, and J. Oh, "Adaptive engagement control of a self-energizing clutch actuator system based on robust position tracking," *IEEE/ASME Transactions on Mechatronics*, 2018.
[8] S. Kim and S. Choi, "Control-oriented modeling and torque estimations for vehicle driveline with dual-clutch transmission," *Mechanism and Machine Theory*, vol. 121, pp. 633–649, 2018.
[9] S. Kim, J. J. Oh, and S. B. Choi, "Driveline torque estimations for a ground vehicle with dual-clutch transmission," *IEEE Transactions on Vehicular Technology*, vol. 67, no. 3, pp. 1977–1989, 2017.
[10] J. Oh, S. Choi, Y. Chang, and J. Eo, "Engine clutch torque estimation for parallel-type hybrid electric vehicles," *International Journal of Automotive Technology*, vol. 18, no. 1, pp. 125–135, 2017.
[11] J. J. Oh and S. B. Choi, "Real-time estimation of transmitted torque on each clutch for ground vehicles with dual clutch transmission," *IEEE/ASME Transactions on Mechatronics*, vol. 20, no. 1, pp. 24–36, 2015.
[12] J. Park, S. Choi, J. Oh, and J. Eo, "Engine net torque compensation through driveline torque estimation in a parallel hybrid vehicle," *International Journal of Automotive Technology*, vol. 20, no. 3, pp. 619–627, 2019.
[13] P. D. Walker and N. Zhang, "Modelling of dual clutch transmission equipped powertrains for shift transient simulations," *Mechanism and Machine Theory*, vol. 60, pp. 47–59, 2013.
[14] Z. Zhao, L. He, Y. Yang, C. Wu, X. Li, and J. K. Hedrick, "Estimation of torque transmitted by clutch during shifting process for dry dual clutch transmission," *Mechanical Systems and Signal Processing*, vol. 75, pp. 413–433, 2016.
[15] X. Zhu, F. Meng, H. Zhang, and Y. Cui, "Robust driveshaft torque observer design for stepped ratio transmission in electric vehicles," *Neurocomputing*, vol. 164, pp. 262–271, 2015.
[16] S. Kim, J. Oh, and S. Choi, "Gear shift control of a dual-clutch transmission using optimal control allocation," *Mechanism and Machine Theory*, vol. 113, pp. 109–125, 2017.
[17] J. Park and S. Choi, "Otimization method of reference slip speed in clutch slip engagement in vehicle powertrain."
[18] B. Gao, H. Chen, Y. Hu, and K. Sanada, "Nonlinear feedforward–feedback control of clutch-to-clutch shift technique," *Vehicle system dynamics*, vol. 49, no. 12, pp. 1895–1911, 2011.
[19] Y. Liu, D. Qin, H. Jiang, and Y. Zhang, "Shift control strategy and experimental validation for dry dual clutch transmissions," *Mechanism and Machine Theory*, vol. 75, pp. 41–53, 2014.
[20] X. Lu, S.-h. Wang, Y.-f. Liu, and X.-y. Xu, "Application of clutch to clutch gear shift technology for a new automatic transmission," *Journal of Central South University*, vol. 19, no. 10, pp. 2788–2796, 2012.
[21] P. D. Walker, N. Zhang, and R. Tamba, "Control of gear shifts in dual clutch transmission powertrains," *Mechanical Systems and Signal Processing*, vol. 25, no. 6, pp. 1923–1936, 2011.
[22] R. I. Davis and R. D. Lorenz, "Engine torque ripple cancellation with an integrated starter alternator in a hybrid electric vehicle: implementation and control," *IEEE Transactions on Industry Applications*, vol. 39, no. 6, pp. 1765–1774, 2003.
[23] S. Hohmann, M. Sackmann, and V. Krebs, "Nonlinear torque control of a spark ignition engine," *IFAC Proceedings Volumes*, vol. 33, no. 9, pp. 591–596, 2000.
[24] T. Huang, D. Liu, H. Javaherian, and N. Jin, "Neural sliding-mode control of engine torque," *IFAC Proceedings Volumes*, vol. 41, no. 2, pp. 9453–9458, 2008.
[25] J. Park, S. Choi, J. Oh, and J. Eo, "Engine indicated torque estimation of a naturally aspired gasoline engine," *International Journal of Automotive Technology*, vol. 21, no. 5, pp. 1195–1205, 2020.
[26] T. Arndt, A. Tarasow, C. Bohn, G. Wachsmuth, and R. Serway, "Estimation of the clutch characteristic map for wet clutch transmissions considering actuator signal and clutch slip," *IFAC-PapersOnLine*, vol. 49, no. 11, pp. 742–748, 2016.
[27] L. Glielmo, L. Iannelli, V. Vacca, and F. Vasca, "Gearshift control for automated manual transmissions," *IEEE/ASME transactions on mechatronics*, vol. 11, no. 1, pp. 17–26, 2006.
[28] H.-S. Jeong and K.-I. Lee, "Friction coefficient, torque estimation, smooth shift control law for an automatic power transmission," *KSME international journal*, vol. 14, no. 5, pp. 508–517, 2000.
[29] ——, "Shift characteristics analysis and smooth shift for an automatic power transmission," *KSME international journal*, vol. 14, no. 5, pp. 499–507, 2000.
[30] J. J. Oh, J. S. Eo, and S. B. Choi, "Torque observer-based control of self-energizing clutch actuator for dual clutch transmission," *IEEE Transactions on Control Systems Technology*, vol. 25, no. 5, pp. 1856–1864, 2017.
[31] J. Park, S. Choi, J. Oh, and J. Eo, "Adaptive torque tracking control during slip engagement of a dry clutch in vehicle powertrain," *Mechanism and Machine Theory*, vol. 134, pp. 249–266, 2019.
[32] A. Tarasow, C. Bohn, G. Wachsmuth, and R. Serway, "Online estimation of 3d-torque characteristics of dual clutches using control oriented models," *IFAC Proceedings Volumes*, vol. 46, no. 21, pp. 452–457, 2013.
[33] A. Bemporad, F. Borrelli, L. Glielmo, and F. Vasca, "Hybrid control of dry clutch engagement," in *2001 European Control Conference (ECC)*. IEEE, Conference Proceedings, pp. 635–639.
[34] X. Lu, P. Wang, B. Gao, and H. Chen, "Model predictive control of amt clutch during start-up process," in *2011 Chinese Control and Decision Conference (CCDC)*. IEEE, Conference Proceedings, pp. 3204–3209.
[35] M. Pisaturo, M. Cirrincione, and A. Senatore, "Multiple constrained mpc design for automotive dry clutch engagement," *IEEE/ASME Transactions on Mechatronics*, vol. 20, no. 1, pp. 469–480, 2014.
[36] L. Wang, *Model predictive control system design and implementation using MATLAB®*. Springer Science & Business Media, 2009.

Jinrak Park received the B.S. degree in automotive engineering from Kookmin University, Seoul, Korea, in 2015, and the M.S. degree in the division of future vehicle from Korea Advanced Institute of Science and Technology (KAIST), Daejeon, Korea, where he is currently working toward the Ph.D. degree in mechanical engineering. His current research interests include automotive powertrain control, automotive transmission control, optimal control of vehicle fuel efficiency and performance, and digital signal processing.

Seibum Choi received the B.S. degree in mechanical engineering from Seoul National University, Seoul, Korea, the M.S. degree in mechanical engineering from the Korea Advanced Institute of Science and Technology (KAIST), Daejeon, Korea, and the Ph.D. degree in control from the University of California, Berkeley, CA, USA, in 1993. From 1993 to 1997, he was involved in the development of automated vehicle control systems at the Institute of Transportation Studies, University of California. During 2006, he was with TRW,Warren, MI, USA, where he was involved in the development of advanced vehicle control systems. Since 2006, he has been with the faculty of the Mechanical Engineering Department, KAIST. His current research interests include fuel-saving technology, vehicle dynamics and control, active safety systems, and ultrasonic applications on a vehicle.